Article

J. Braz. Chem. Soc., Vol. 22, No. 1, 21-29, 2011.
Printed in Brazil - ©2011 Sociedade Brasileira de Química
0103 - 5053 $6.00+0.00

Epicarp and Mesocarp of Babassu (*Orbignya speciosa*): Characterization and Application in Copper Phtalocyanine Dye Removal

Adriana P. Vieira,[a] Sirlane A. A. Santana,*,[a] Cícero W. B. Bezerra,[a] Hildo A. S. Silva,[a] José A. P. Chaves,[b] Júlio C. P. de Melo,[c] Edson C. da Silva Filho[d] and Claudio Airoldi[c]

[a]Departamento de Química/CCET, Universidade Federal do Maranhão, Avenida dos Portugueses S/N, Campus do Bacanga, 65080-540 São Luís-MA, Brazil

[b]Colégio Universitário, Universidade Federal do Maranhão, 65080-540 São Luís-MA, Brazil

[c]Institute of Chemistry, University of Campinas, CP 6154, 13084-971 Campinas-SP, Brazil

[d]Química, Campus Amilcar Ferreira Sobral, Universidade Federal do Piauí, 64800-000 Floriano-PI, Brazil

Os componentes mesocarpo e epicarpo do coco babaçu foram utilizados como novos biossorventes alternativos para remoção do corante têxtil ftalocianina de cobre de soluções aquosas. Esses biopolímeros foram caracterizados por análise elementar, RMN de ^{13}C no estado sólido, espectroscopia de absorção na região do infravermelho, análise termogravimétrica e difratometria de raios X. Os resultados mostraram que a composição do mesocarpo e do epicarpo é similar à de outros materiais lignocelulósicos e que ambos os componentes são efetivos na remoção do corante têxtil Turqueza Remazol. O modelo cinético de pseudo-segunda ordem resultou no melhor coeficiente de correlação tanto para o epicarpo quanto para o mesocarpo (R^2 = 0,999), com constantes de velocidade de sorção, k_2, de 0,31 e 1,43 g mg^{-1} min^{-1}, respectivamente. Os modelos de Langmuir e Freundlich foram empregados para analisar os dados experimentais em sua forma linearizada. O segundo modelo apresentou melhor adequação para a adsorção do corante Turqueza Remazol com sorção máxima de 1,44 e 2,38 mg g^{-1} a pH 6,0 para mesocarpo e epicarpo, respectivamente.

The mesocarp and epicarp components of the babassu palm tree were applied as novel alternative biosorbents for copper phtalocyanine textile dye removal from aqueous solutions. The natural biopolymers were characterized by elemental analyses, solid state ^{13}C NMR, infrared spectroscopy, thermogravimetric analysis and X-ray diffractometry. Results demonstrated that the compositions of the mesocarp and epicarp are similar to those of other lignocellulosic materials, and that they were very effective for removal of the textile dye Turquoise Remazol. A pseudo second-order kinetic model resulted in the best fit with experimental data for both epicarp and mesocarp (R^2 = 0.999), providing rate constants of sorption, k_2, of 0.31 and 1.43 g mg^{-1} min^{-1}, respectively. The Langmuir and Freundlich isotherm models were employed for adsorption analysis of the experimental data in their linearized forms. The second model resulted in the better fit for Turquoise Remazol dye, which presented maximum adsorption of 1.44 and 2.38 mg g^{-1} at pH 6.0 for mesocarp and epicarp, respectively.

Keywords: mesocarp, epicarp, babassu coconut, adsorption, dye textile

Introduction

Environmental pollution, in general, is one of the most serious problems confronted by society and is directly linked to industrial development, with textile activities being responsible for the worsening of the situation, generating a considerable amount of colored wastewater.[1] It is estimated that around 15% of the world's production of dyes is lost to the environment during synthesis, processing and applications.[2] From the environmental point of view this is a serious problem, since the disorderly dumping of effluents into aquatic environments such

*e-mail: sirlane@ufma.br

as rivers, streams and lakes, without prior treatment, decreases the transparency of water and the penetration of solar radiation, affecting photosynthetic activity and solubility of gases and causing serious damage to regional fauna and flora.[3]

Conventional methods used for dye removal from industrial effluents include biodegradation, Fenton and photo-Fenton oxidations, electroflocculation, combined photo catalytic and ozonation processes, adsorption, etc. However, some of these processes may form intermediate compounds with higher degrees of toxicity, as happens with ozone, which makes it necessary to monitor the process through toxicity tests.[4] In addition, most of these methods are often expensive or ineffective, especially for dye removal from dilute solutions.

The adsorption is an efficient treatment process for dye removal from wastewater.[5] The first step for an effective process of adsorption is the choice of a sorbent with high capacity and long life, available on a large scale and at low cost. It is considered low cost if it requires little processing, is naturally abundant or is a by-product or waste from another industry.[6] Normally, the adsorption process is studied on the basis of empirical models such as Langmuir and Freundlich. The first model assumes that the sorbent surface is covered by adsorption sites with identical energies and each sorbed molecule adheres to a single site, predicting the formation of a sorbate monolayer on the surface.[7] On the other hand, the Freundlich model describes a reversible heterogeneous adsorption without restricting the covering to forming a monolayer on the sorbate.[8]

Investigations have recently been directed to alternative sorbents, also known as low-cost or unconventional, based on both the environmental and the economical points of view.[9-20] In order to overcome high cost problems, an increasing interest in producing new alternative sorbent materials to replace the most used activated carbon has been raised, also taking into account local availability, since these new materials are frequently constituted of residues from agricultural activity or sea food processing.[21]

Brazil has a high potential for lignocellulosic fiber production. As an example, this type of material results from babassu (*Orbignya speciosa*) biomass, a very abundant palm tree in the north-central region of the country, especially in the State of Maranhão. The babassu palm tree is of large size, up to 20 m, having a cylindrical trunk with a crown containing a number of fruits in ellipsoidal form. Each fruit is constituted of epicarp, mesocarp, endocarp and almond with 11, 23, 59 and 7% in mass, respectively.[22]

The major exploitation of the babassu almond is for lauric oil production, which can be used for energetic purposes, such as biodiesel production, or in cooking.[23-25] The most common use for the epicarp is coal production due to its stiffness, while the mesocarp is used by food ration manufacturers, since it is rich in sugars and, consequently, can be useful in nutritional compositions.[21] Normally, most extractive processes consist in collecting the attractive almonds from the fruits, leaving all the other components unexploited.

Recent research has analyzed other applications of the outer layers of the babassu, including the anti-inflammatory and analgesic properties[26-29] of the mesocarp, which is also capable of adsorbing various textile industry dyes.[30] Also, the structural features associated with mesocarp and epicarp permit their use as polymeric supports for the immobilization of ethylenesulfide followed by divalent cation removal from aqueous solutions.[31]

From the environmental point of view, there is some difficulty in color removal from solutions of metallated dyes often encountered in wastewater. For example, copper may be released during the process, and this metal is controlled by environmental regulations. Studies have usually been related to decoloration of azo dyes, which are currently of wide use in the textile industry, with the exclusion of other commercially important classes of textile dyes such as the metallophtalocyanines. Photochemical oxidation has been employed for removal of the latter; however, the method is limited at high dye concentration.[32]

Taking into account the great availability of the byproducts of *Orbignya speciosa* after extraction of the almonds, the present investigation deals with the characterization and evaluation of the mesocarp and epicarp of babassu as sorbents for copper phtalocyanine, the agent in the textile dye Turquoise Remazol, from aqueous solutions. These studies are directly related to the potential uses of abundant, naturally growing palm trees in northeastern Brazil. In this context, the babassu tree is of great importance and the use of its byproducts can contribute to the expected sustainable development of that geographical region.

Experimental

Materials and reagents

The mesocarp and epicarp components were extracted from raw babassu fruits acquired in the city of São Luís, Maranhão state, Brazil. The individual parts were used after crushing the raw material into particle sizes in the 0.088-0.177 mm range. The dye Turquoise Remazol, CI 74160, shown in Figure 1, was supplied by Indústria de Toalhas de São Carlos, located in the state of São Paulo, Brazil. The

chemical reagents NaOH, HCl, KCl, potassium biphtalate ($C_8H_5O_4K$) and $Na_2B_4O_7{\cdot}10H_2O$ were all of analytical grade. Microcrystalline cellulose as powder (Aldrich), *ca.* 20 μm, was used as a reference biopolymer during the characterization of the materials studied in this work.

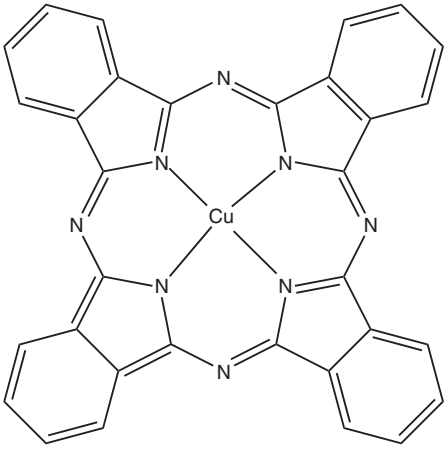

Figure 1. Chemical structure of the Turquoise Remazol dye.

Biomass characterization

Infrared spectra were obtained in the 4000 to 400 cm^{-1} range by accumulating 32 scans on a MB-Bomem FTIR spectrophotometer using KBr pellets with a resolution of 4 cm^{-1}. Elemental analyses were performed with a Perkin-Elmer 2400 Series II equipment. Thermogravimetric curves (TG) for the powdered samples were obtained out with a Shimadzu TGA-50 instrument under a nitrogen flow rate of 30 cm^3 min^{-1}, in the temperature interval from 298 to 1000 K, with a heating rate of 10 K min^{-1} and initial sample mass of 10.0 mg. ^{13}C NMR spectra in the solid state were obtained on a Bruker AC 400/P spectrometer, by using the frequency of 75.47 MHz with a magic angle spinning of 10 Hz. X-ray diffraction patterns were recorded using a Shimadzu XD3-A diffractometer for the powdered samples with Cu-K_α radiation, $\lambda = 1.5418$ nm, at 30 kV, 20 mA and 2θ angular regions in the 5 to 50° range. The pH measurements were obtained by using DM-21 Digimed instrument.

Adsorption

The ability of the surfaces to extract the textile dye Turquoise Remazol from doubly distilled water solutions was evaluated by measuring adsorption isotherms at pH 6.0. The variation of adsorption as a function of pH (from 1.0 to 13.0) was analyzed by using appropriate buffer solutions. Under equilibrium conditions, the exchange processes at the solid/liquid interface can be characterized by the amount (mg) sorbed per gram of support. The batchwise adsorption experiments were carried out under stirring at 298 ± 1 K, by using *ca.* 100 mg of mesocarp or epicarp suspended in 10.0 cm^3 of aqueous solutions with dye concentrations varying from 13.6 to 54.4 mg dm^{-3}. The suspensions were shaken for 60 min and the required time was established from prior experiments to ensure maximum sorption. At the end of this process, the solid was separated by filtration and the concentration of the dye sorbed by the biomass was determined by difference between the initial concentration of the aqueous solution and that found in the supernatant, by using a Varian AA 50 spectrophotometer at a wavelength of 620 nm.

The amount of dye adsorbed,[15] q_e (mg g^{-1}), was calculated with equation 1:

$$q_e = \frac{C_i - C_f}{W} \times V \quad (1)$$

where C_i and C_f are the initial and final dye concentrations at equilibrium in the aqueous phase (mg dm^{-3}), respectively, V is volume of dye solution (dm^3) and W (g) is the amount of mesocarp or epicarp employed.

The proposed mechanism of adsorption was investigated by fitting the results of the kinetic data to pseudo first and second-order reactions,[33] as given by equations 2 and 3 respectively.

$$\log(q_e - q_t) = \log q_e - \frac{k_1}{2.303} \times t \quad (2)$$

$$\frac{t}{q_t} = \frac{1}{k_2 q_e^2} + \frac{1}{q_e} \times t \quad (3)$$

where q_e and q_t are the amounts of dye sorbed (mg g^{-1}) at equilibrium and at time t, respectively, k_1 (min^{-1}) is the rate constant of first-order adsorption and k_2 (g mg^{-1} min^{-1}) is the rate constant of second-order sorption.

The Langmuir and Freundlich isotherm models were employed to analyze the experimental adsorption data in their linearized forms,[34] equations 4 and 5 respectively. The isotherm model chosen was that whose linearization provided the best fit to experimental data, that is, the best correlation coefficient value (R).

$$\frac{C_e}{q_e} = \frac{1}{q_{\max} K_{ads}} + \frac{C_e}{q_{\max}} \quad (4)$$

$$\log q_e = \frac{\log C_e}{n} + \log K_f \quad (5)$$

where C_e is the dye concentration at equilibrium, q_e is the amount of dye adsorbed, q_{max} is the maximum adsorption capacity, K_{ads} is the Langmuir constant, and n and K_f are Freundlich constants.

Results and Discussion

Biomass characterization

Elemental analysis gave for mesocarp 39.23, 6.70, 0.33; epicarp 46.72, 6.12, 0.51 and cellulose 41.95, 6.21, 0.18% for carbon, hydrogen and nitrogen, respectively. These results show that the mesocarp and epicarp biopolymers obtained from low cost babassu byproducts have elemental compositions close to that of cellulose.

The infrared spectra for cellulose, mesocarp and epicarp are presented in Figure 2. Cellulose, as shown in Figure 2 (a), presented bands attributed to H-bonded OH groups at 3400 to 3300 cm^{-1}. The stretching bands of CH_2 and CH_3 appear in the 2800 to 3000 cm^{-1} interval. The band at 1639 cm^{-1} corresponds to δ(O-H) of the hydroxyl groups of the cellulose structure and those between 1200 to 1000 cm^{-1} are related to ν(C-O).[35] The spectra of mesocarp and epicarp are shown in Figures 2 (b) and (c), respectively. The most remarkable differences between the mesocarp and the cellulose spectra are at 860, 769 and 710 cm^{-1}, where the bands related to vibrations of esters and monosubstituted aromatic rings due to the lignin fraction of the material are recorded. For epicarp, the most significant differences are at 1740 cm^{-1}, ν(C=O) for carboxylic esters, and at 1650 cm^{-1}, ν(C-OH) for alcohol groups, also due to the presence of lignin. The bands around 1610-1460 cm^{-1} refer to ν(C=C) of aromatic rings, aromatic skeletal vibrations, aromatic ring deformation and –CHO out of plane vibrations. Similar bands to those found in cellulose at 1248 cm^{-1} are attributed to ν(C–O–C) and at 1161 cm^{-1} are associated with the β-1,4 linkage. Based on the appearance of this broad band it is inferred that an overlap occurred involving ν(C-O), ν(C-C) and ν(C-H) aromatic bending vibrations. The bands associated with tetra- and trisubstituted benzene out of plane vibrations[36] are assigned at 853 and 772 cm^{-1}, respectively.

The solid state ^{13}C NMR spectra for cellulose (a), mesocarp (b) and epicarp (c) are shown in Figure 3. As observed, both babassu components present similar sets of peaks in the spectra when compared to cellulose. The polysaccharide carbon 1 signal was attributed at 104 ppm, taking into account that it is bonded to two electronegative oxygen atoms, as shown in Figure 3 (a). For carbon 4 two distinct peaks are available at 88 and 83 ppm, which were attributed to the carbon associated with crystalline and amorphous regions, as normally occurs with the morphology of pure cellulose.[37] Carbons 2, 3 and 5, with almost equivalent chemical environments, were attributed to the signals at 71 to 75 ppm. The peaks with small chemical shifts between 64 and 62 ppm were assigned to carbon 6 in the crystalline and amorphous regions,[35] respectively.

In the mesocarp spectrum, as shown in Figure 3 (b), there is a small difference for carbon 4, which is responsible for the 1,4'-β-glucosidic linkage. In this case, only one signal at 83 ppm is recorded, in agreement with the existence of the crystalline form of the cellulosic component. The epicarp spectrum is affected by the presence of a higher amount of lignin in this part of the babassu fruit, as shown in Figure 3c. A clear difference is observed by the signal at 22 ppm, which is related to methyl groups due to lignin. Several other small signals emerged when compared to cellulose, all of them due to chemical shifts of the carbonic lignin structure, such as the signals at 116 to 120, 133 and 149 to 153 ppm, assigned to aromatic carbons. The broad signals at 160 and 178 ppm correspond to aldehydes, ketones and esters, also originating from the complex structure of the lignin.[38]

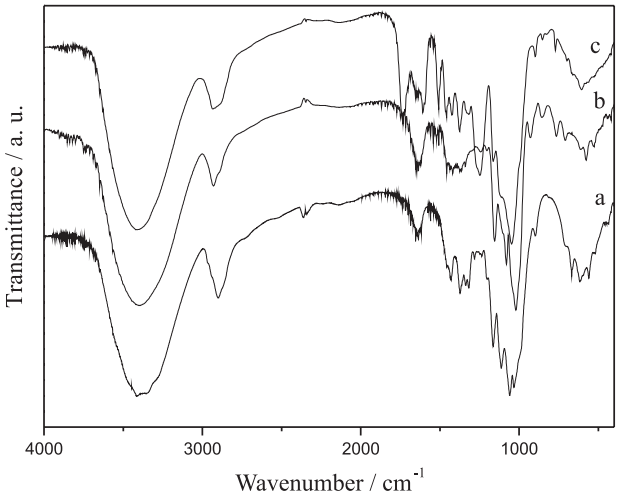

Figure 2. FTIR spectra of cellulose (a) and of the mesocarp (b) and epicarp (c) of babassu fruit.

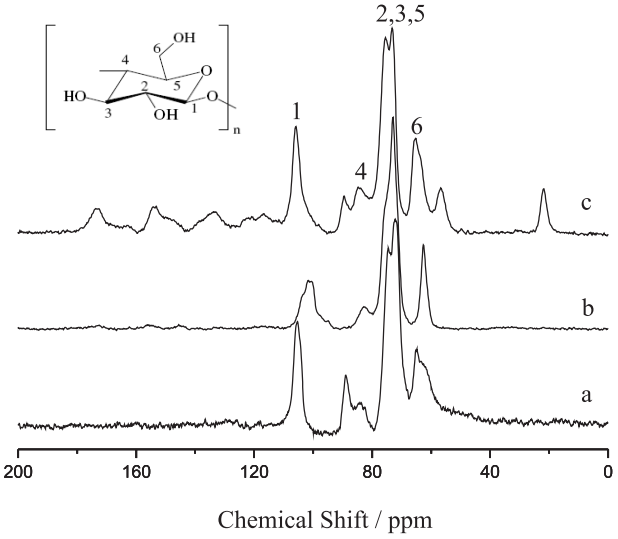

Figure 3. ^{13}C NMR spectra of cellulose (a), and of the mesocarp (b) and epicarp (c) of babassu fruit.

X-ray diffraction patterns for cellulose and the lignocellulosic components are shown in Figure 4. The diffractogram for cellulose, as shown in Figure 4 (a), is similar to that given by the epicarp, in Figure 4 (c). In fact, the diffraction pattern in 4c probably come from the cellulosic constituents, as observed for a main peak at about $2\theta = 22^{o}$. For mesocarp, Figure 4 (b), the principal difference is related to two peaks around 16^{o}. In the two babassu components, two peaks are noted in this region when the cellulose content is high, but when the fiber contains an increased amount of amorphous components such as lignin, hemicelluloses and amorphous cellulose, the two peaks are smeared and appear as a single broad feature like that shown for epicarp in Figure 4 (c).[36]

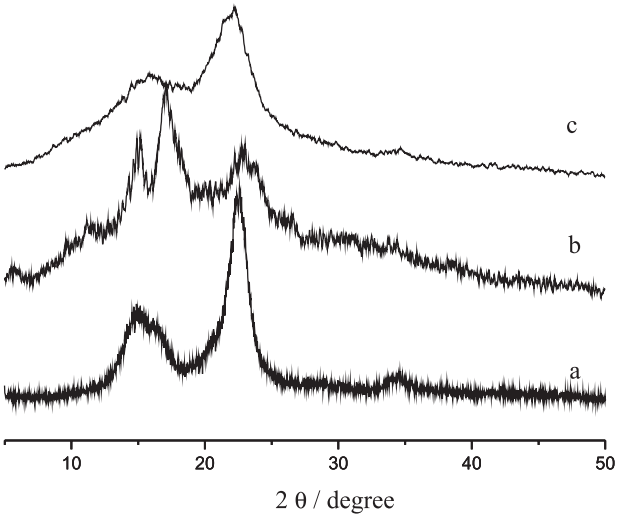

Figure 4. X-ray diffraction patterns of cellulose (a), and of the mesocarp (b) and epicarp (c) of babassu fruit.

The thermogravimetric curves obtained in an inert atmosphere for cellulose, mesocarp and epicarp are shown in Figure 5. Cellulose gave only one event in the decomposition process covering the interval of temperature from 536 to 647 K, corresponding to a mass loss of 92%.[35] For mesocarp the first stage, up to 375 K, corresponds to the mass loss of 12%, followed by another mass loss of 62% in the 477 to 623 K interval. Epicarp showed mass losses of 11% at 353 K and of 56% between 609 and 638 K, for the same experimental conditions. The first step of decomposition can be attributed to the release of low mass carbon-rich molecules and sorbed water, while the second stage is due to the decomposition of organic material, for example breakdown of fibers with caramel and graphene formation, resembling other lignocellulosic materials whose main components are cellulose, lignin and hemicelluloses.[36,39]

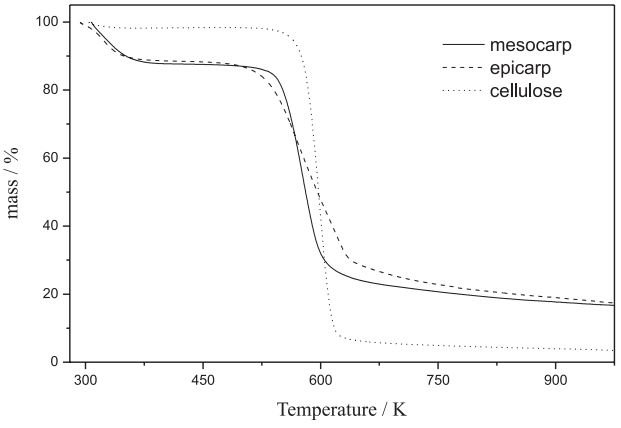

Figure 5. TGA curves obtained for cellulose and for the mesocarp and epicarp of the babassu fruit in an inert atmosphere.

Adsorption

The curves of adsorption of Turquoise Remazol dye by mesocarp and epicarp as a function of time are shown in Figure 6. For these materials, the adsorption process reached equilibrium in 20 and 60 min, respectively,

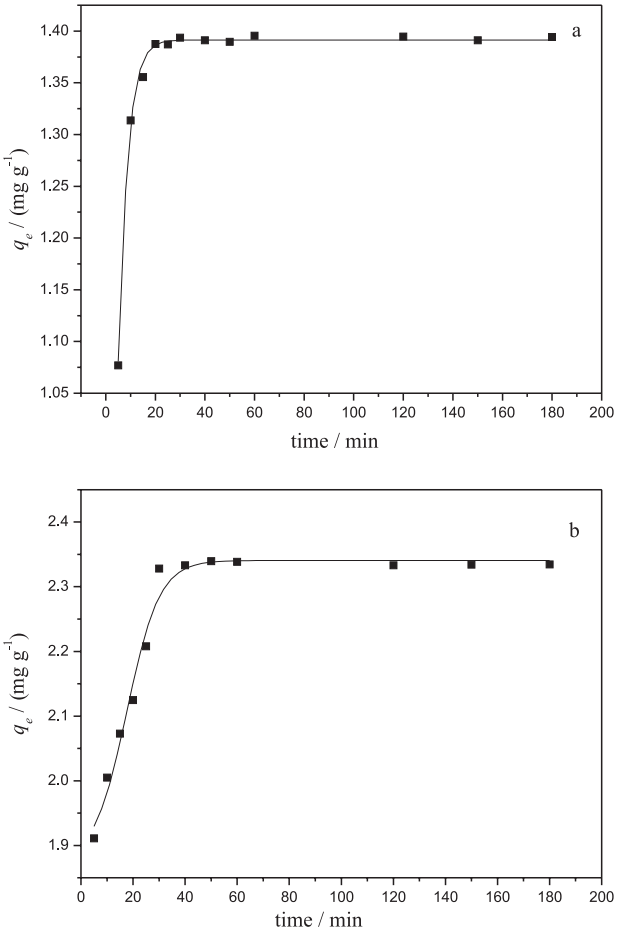

Figure 6. Kinetics of the adsorption of Turquoise Remazol onto mesocarp (a) and epicarp (b) of babassu fruit at 298 ± 1 K and pH 6.0.

remaining constant for 3 h. The adsorption data were fitted to pseudo first-order and pseudo second-order kinetic models. The pseudo first-order model presented lower linear correlation coefficients for mesocarp and epicarp (results not shown), with q_e values of 0.03 and 0.17 mg g^{-1}, with greater discrepancy in relation to the experimental q_e values.

The best correlation coefficients for mesocarp (R = 0.999) and epicarp (R = 0.999) were provided by the pseudo second-order model, indicating chemisorption as the determinant stage in the adsorption mechanism, as shown in Figure 7. The results obtained with the pseudo second-order model are shown in Table 1, which gives the rate constants k_2 of 1.43 and 0.31 g mg^{-1} min^{-1} for mesocarp and epicarp, respectively.

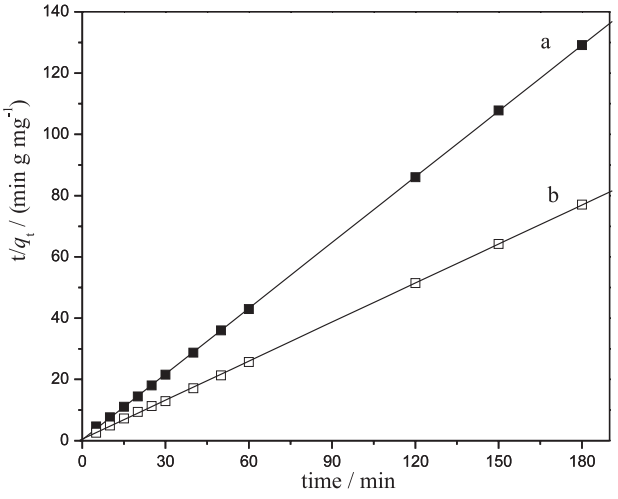

Figure 7. Pseudo-second order model curve for the adsorption of Turquoise Remazol onto mesocarp (a) and epicarp (b) of babassu fruit.

The q_e values obtained from equation 3 and the slopes of 1.40 and 2.36 mg g^{-1} demonstrated good agreement with the experimental values of 1.44 and 2.38 mg g^{-1}. From the k_2 and q_e values, the initial adsorption rates (h) were determined as 2.8 and 1.7 mg g^{-1} min^{-1} by equation 6. Thus, the initial adsorption on mesocarp was nearly two times greater than on epicarp.

$$h = k_2 \times q_e^2 \quad (6)$$

The kinetics of adsorption of many dyes onto various materials is frequently found to be of second-order.[30] The applicability of the pseudo second-order model suggests that chemisorption might be the rate-limiting step that controls the adsorption processes. In general, this model has the following advantage: the adsorption capacity, the pseudo second-order rate constant and the initial adsorption rate can be determined.[40]

The adsorption isotherm represents the concentrations of dye sorbed at equilibrium (q_e) according to the amount adsorbed per gram of sorbent. Profiles of the isotherm of Turquoise Remazol adsorption from aqueous solution on mesocarp and epicarp are shown in Figure 8.

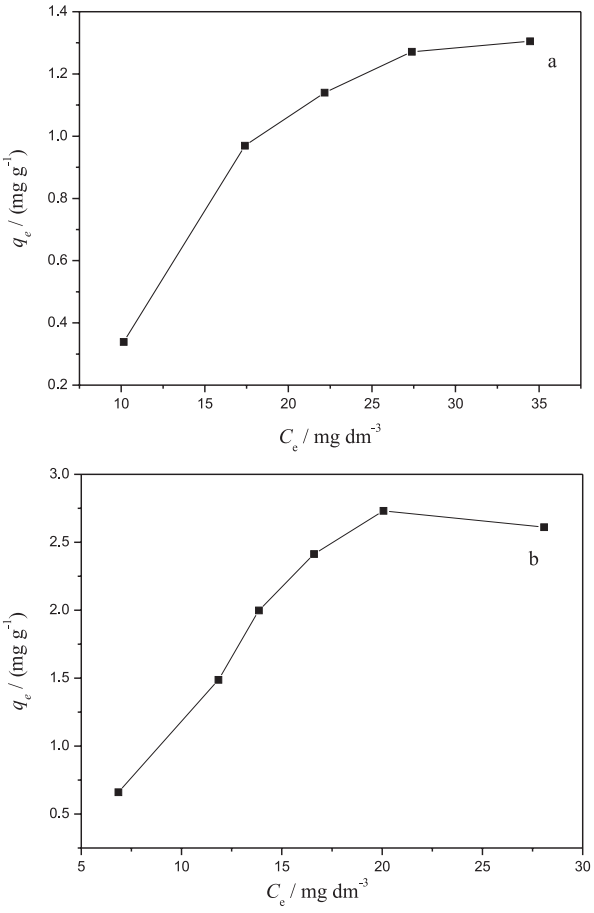

Figure 8. Isotherm of Turquoise Remazol adsorption onto mesocarp (a) and epicarp (b) of babassu fruit at 298 ± 1 K and pH 6.0.

Table 1. Kinetic parameters determined for Turquoise Remazol adsorption onto mesocarp and epicarp of the babassu coconut using pseudo first-order and pseudo second-order equations

Biomass	$q_{e,exp}$/(mg g^{-1})	Pseudo First-order			Pseudo Second-order			
		$k_1 \times 10^2$ / min^{-1}	q_e / (mg g^{-1})	R^2	k_2 / (g mg^{-1} min^{-1})	q_e / (mg g^{-1})	R^2	h / (mg g^{-1} min^{-1})
Mesocarp	1.44	2.1	0.03	0.701	1.43	1.40	0.999	2.8
Epicarp	2.38	2.7	0.17	0.766	0.31	2.36	0.999	1.7

From the adsorption curves the plateau was progressively approached as the concentration investigated increased. Thus, the maximum quantity of the dye sorbed by these matrices was 1.44 and 2.38 mg g^{-1} for mesocarp and epicarp, respectively.

Analyses of correlation coefficients showed that the Freundlich isotherm provided the best fit for experimental data for both epicarp and mesocarp. The results are listed in Table 2, which was obtained from linearizations following the Freundlich model (Figure S1, Electronic Supplementary Information). The parameters n and K_f, the constants of the system, which act as indicators of adsorption capacity and intensity, respectively, were determined from the intercept and the slope of the straight line equation obtained by plotting log q_e versus log C_e.

Table 2. Parameters determined from Freundlich isotherms for adsorption onto the mesocarp and epicarp of babassu fruit

Biomass	n	K_f	R^2
Mesocarp	0.90	0.03	0.931
Epicarp	0.96	0.11	0.923

The results from the Langmuir model presented a poor linear fit for dye adsorption on both epicarp and mesocarp. Babassu mesocarp and fly ash, as low-cost sorbents, have been investigated for the removal of several dyes. The results obtained also indicated that the Freundlich adsorption isotherm fit the data better than the Langmuir analogue.[30,41] Calcium-rich fly ash was studied for the adsorption of Congo Red from aqueous solution and the author reported that the adsorption process obeyed the pseudo second-order kinetic model and the adsorption isotherm followed the Freundlich model.[42] On the other hand, the adsorption of Brilliant Green on Neem leaf powder yielded good fits with the Langmuir isotherm as well as the empirical Freundlich isotherm.[43] However, the Freundlich equation was preferred for the description of the isotherms of reactive dyes although the isotherms of acidic and basic dyes were better fitted by the Langmuir model, depending on the dye concentration. These investigations confirm that the empirical Freundlich equation is applicable to the adsorption of single solutes within a fixed range of concentration.[8]

Effect of pH

The adsorption of Turquoise Remazol by the mesocarp and epicarp of babassu increases considerably as the acidity is increased, as shown in Figure 9.

According to these results, the optimal sample pH for dye removal is apparently 1.0. In this condition,

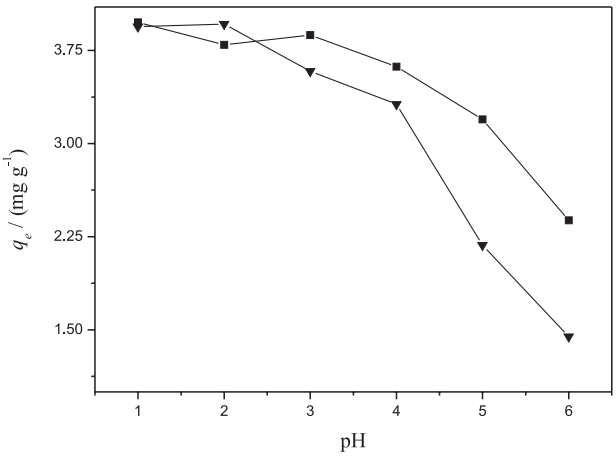

Figure 9. Effect of pH on the adsorption of Turquoise Remazol dye onto mesocarp (▼) and epicarp (■) of babassu fruit at 298 ± 1 K.

the maximum quantities of the dye sorbed were 3.94 and 3.97 mg g^{-1}, which correspond to 96.6 and 99.5% for mesocarp and epicarp, respectively. Although the adsorption at pH 6.0 gave lower values of 1.44 and 2.38 mg g^{-1}, it seems the more appropriate condition for applications to normal aqueous solutions.

A similar trend was observed for the adsorption of Direct Red onto banana pith,[44] which had a maximum removal of 80% at an initial pH of 3.0. For Congo Red adsorption on coir pith two possible mechanisms for the effect of pH were proposed: (a) electrostatic interaction between the possible unprotonated groups and the acidic dye and (b) chemical reaction between the sorbate and the sorbent.[45] Similar results of pH effect were also reported for the adsorption of Acid Yellow 36 and Reactive Red 189.[46-48]

The main components of the mesocarp and epicarp are cellulose, lignin and hemicelluloses. These natural products contain a large number of functional groups, including phenolic OH as well as carboxylic groups. The interaction of the dye molecules with these functional groups may follow an extremely complicated pattern. As the pH of the system decreases, the number of negatively charged surface sites also decreases, with a consequent increase of the number of positive sites on the same surface, which favors the adsorption of anionic dyes due to electrostatic attraction, as is expected for the electroneutralization process.

As mentioned previously, lignocellulosic materials have been studied extensively as sorbents for dye removal. However, there is still much to be accomplished in understanding the mechanisms. In particular, dye molecules have many different and complicated structures and this is one of the most important factors that influence adsorptions and their mechanisms.[1,5] However, some suggestions are made by taking into account the biopolymer composition and the chromophores to be sorbed. As

reported here, in mesocarp and epicarp of the babassu fruit the major functional groups are capable of establishing interactions such as hydrogen bonds and aromatic ring π-π interactions, as well as van der Waals interactions. Here the establishment of hydrogen bonds between protons or non-bonding electron pairs on lignocellulosic material with the available π electrons of the double bond or the acidic centers on dyes is proposed. Another possibility is to consider that the aromatic rings present in the lignin may interact with the acidic copper located in the dye structure of Turquoise Remazol.

Conclusions

X-ray diffraction studies showed that the mesocarp and epicarp components obtained from babassu fruits present a low crystallinity fraction, as observed for other lignocellulosic materials. This result is also supported by ^{13}C NMR data, where mesocarp signals present chemical shifts similar to those attributed to cellulose, while epicarp shows characteristic lignin signals. Thermal analysis of the fibers revealed that the degradation processes occur according to their cellulose, hemicellulose and lignin constituents. FTIR studies reveal structural features such as O–H and C–H stretching that are characteristic of the chemical fractions of the materials, which can sorb Turquoise Remazol dye in a process that depends on pH. The kinetics of adsorption is described by the pseudo second-order model and the isotherms fit the Freundlich model. Based on the significant adsorption capacity shown by this new material for Turquoise Remazol removal, it can then be proposed as an alternative inexpensive sorbent from aqueous solutions. On the other hand, the adsorption capacity was higher for epicarp, suggesting possible selectivity due to its higher quantities of available functional groups. Taking into account this set of results, it is reasonable to infer that the babassu fruit components may have many potential applications in dye removal. Additional studies are required to fully exploit this possibility, resulting in significant social benefits.

Supplementary Information

Supplementary data are available free of charge at http://jbcs.sbq.org.br, as PDF file.

Acknowledgments

The authors acknowledge CAPES for financial support, the Indústria de Toalhas São Carlos for the gift of the dye sample, FAPEMA for a fellowship to A. P. V. and CNPq for a fellowship to C. A.

References

1. Crini, G.; *Bioresour. Technol*. **2006**, *97*, 1061.
2. Guarantini, C. I.; Zanoni, M. V. B.; *Quim. Nova* **2000**, *23*, 71.
3. McKay, G.; Otterburn, M. S.; Aga, D. A.; *Water Air Soil. Pollut*. **1985**, *24*, 307.
4. Langlais, B.; Legube, B.; Beuffe, H.; Doré, M.; *Water Sci. Technol*. **1992**, *25*, 135.
5. Gupta, V. K.; Suhas; *J. Environ. Managem*. **2009**, *90*, 2313.
6. Figueiredo, S. A.; Boaventura, R. A.; Loureiro, J. M.; *Sep. Purif. Technol*. **2000**, *20*, 129.
7. Langmuir, I.; *J. Am. Chem. Soc.* **1916**, *38*, 2221.
8. Freundlich, H. M. F.; *Z. Phys.* **1906**, *57A*, 385.
9. Lima, I. S.; Ribeiro, E. S.; Airoldi, C.; *Quim. Nova.* **2006**, *29*, 501.
10. Özacar, M.; Sengil, A. I.; *Bioresour. Technol*. **2005**, *96*, 791.
11. Chuah, T. G.; Jumasiah, A.; Azni, I.; Katayon, S.; Choong, S. T. Y.; *Desalination* **2005**, *175*, 305.
12. Morais, L. C.; Freitas, O. M.; Gonçalves, E. P.; Vasconcelos, L. T.; González Beça, C. G.; *Water Res*. **1999**, *33*, 979.
13. Arami, M.; Limaee, N. Y.; Mahmoodia, N. M.; Tabrizi, N. S.; *J. Hazard. Mater*. **2006** *B135***,** 171.
14. Crini, G.; *Prog. Polym. Sci*. **2005**, *30*, 38.
15. Cestari, A. R.; Vieira, E. R. S.; Santos, A. G. P.; Mota, J. A.; Almeida, V. P.; *J. Colloid Interface Sci.* **2004**, *280*, 380.
16. Poots, V. J. P.; McKay, G.; Healy, J. J.; *Water Res*. **1976**, *10*, 1061.
17. Kamel, M. M.; Magda, M. K.; Youseef, B. M.; Waly, A.; *Am. Dyestuff Rep*. **1991**, *80*, 34.
18. Robinson, T.; Chandran, B.; Nigam, P.; *Environ. Int*. **2002**, *28*, 29.
19. Bhattacharyya, K. G.; Sharma, A.; *Dyes Pigm*. **2005**, *65*, 51.
20. Pirillo S.; Pedroni V.; Rueda E.; Ferreira, M. L.; *Quim. Nova*. **2009**, *32*, 1239.
21. Lima, E. C.; Royer, B.; Vaghtti, J. C. P.; Simon, N. M.; Cunha, B. M.; Pavan, F. A.; Benvenutti, E. V.; Cataluña-Veses, R.; Airoldi, C.; *J. Hazard. Mater*. **2008**, *155*, 536.
22. Albiero, D.; Maciel, A. J. S.; Lopes, A. C.; Mello, C. A.; Gamero, C. A.; *Acta Amaz.* **2007**, *37*, 337.
23. Teixeira, M. A; *Biomass Bioenergy* **2008**, *32*, 857.
24. Teixeira, M. A.; Carvalho, M. G.; *Energy* **2007**, *32*, 999.
25. Freitas, L.; Da Ró, P. C. M.; Santos, J. C.; Castro, H. F.; *Process Biochem.* **2009**, *44*, 1068.
26. Silva, B. P.; Parente, B. P.; *Fitoterapia* **2001**, *72*, 887.
27. Batista, C. P.; Torres, O. J. M.; Matias, J. E. F.; Moreira, A. T. R.; Colman, D.; Lima, J. H. F.; Macri, M. M.; Rauen Jr, R. J.; Ferreira, L. M.; Freitas, A. C. T.; *Acta Cir. Bras.* **2006**, *21*, 26.
28. Azevedo, A. P. S.; Farias, J. C.; Costa, G. C.; Ferreira, S. C. P.; Aragão-Filho, W. C.; Sousa, P. R. A.; Pinheiro, M. T.; Maciel, M. C. G.; Silva, L. A.; Lopes, A. S.; Barroqueiro, E. S. B.; Borges, M. O. R.; Guerra, R. N. M.; Nascimento, F. R. F.; *J. Ethnopharm.* **2007**, *111*, 155.

29. Brito Filho, S. B.; Matias, J. E. F.; Stahlke Júnior, H. J.; Torres, O. J. M.; Timi, J. R. R.; Tenório, S. B.; Tâmbara, E. M.; Carstens, Â. G.; Campos, R. V.; Myamoto, M.; *Acta Cir. Bras.* **2006**, *21*, 76.
30. Vieira, A. P.; Santana, S. A. A.; Bezerra, C. W. B.; Silva, H. A. S; Chaves, J. A. P.; Melo, J. C. P.; da Silva Filho, E. C.; Airoldi, C.; *J. Hazard. Mater*. **2009**, *166*, 1272.
31. Santana, S. A. A.; Vieira, A. P.; da Silva Filho, E. C.; Melo, J. C. P.; Airoldi, C.; *J. Hazard. Mater*. **2010**, *174*, 119.
32. Osugi, M. E; Umbuzeiro, G. A.; Anderson, M. A.; Zanoni, M. V. B.; *Electrochim. Acta* **2005**, *50*, 5261.
33. Allen, S. J.; Gan, Q.; Matthews, R.; Johnson, P. A.; *J. Colloid Interface Sci*., **2005**, *286*, 101.
34. Alley, E. R.; *Water Quality Control Handbook*, McGraw Hill: New York, 2000, p.125.
35. da Silva Filho, E. C.; de Melo, J. C. P.; Airoldi, C.; *Carbohydr. Res*. **2006**, *341*, 2842.
36. Tserki, V.; Matzinos, P.; Kokkou, S.; Panayiotou, C.; *Composites A*, **2005**, *36*, 965.
37. Melo, J. C. P.; da Silva Filho, E. C.; Santana, S. A. A.; Airoldi, C.; *Colloids Surf. A*, **2009**, *346*, 138.
38. Pavia, D. L.; Basser, G. M.; Morrill, T. C.; *Introduction to Spectroscopy*, 2nd ed., Saunders College: New York, 1996.
39. Satyanarayana, K. G.; Guimarães, J. L.; Wypych, F.; *Composites A* **2007**, *38*, 1694.
40. Ho, Y. S.; *J. Hazard. Mater*. **2006**, *B136,* 681.
41. Mohan, D.; Singh, K. P.; Singh, G.; Kumar, K.; *Ind. Eng. Chem. Res*. **2002**, *41*, 3688.
42. Acemioglu, B.; *J. Colloid Interface Sci*. **2004**, *274*, 371.
43. Bhattacharyya, K. G.; Sarma, A.; *Dyes Pigm*. **2003**, *57*, 211.
44. Namasivayam, C.; Prabha, D.; Kumutha, M.; *Bioresour. Technol*. **1998**, *64*, 77.
45. Namasivayam, C.; Kavitha, D.; *Dyes Pigm*. **2002**, *54*, 47.
46. Yuzhu, F.; Viraraghavan, T.; *Adv. Environ. Res*. **2002**, *7*, 239.
47. Malik, P. K.; *Dyes Pigm*. **2003**, *56*, 239.
48. Chiou, M. S.; Li, H. Y.; *J. Hazard. Mater.* **2002**, *B93,* 233.

Submitted: March 3, 2010
Published online: July 22, 2010

FAPESP has sponsored the publication of this article.